Supporting Information

Structure regulation induced high capacity and ultra-stable cycling of conjugated organic cathodes for Li-ion batteries

Xian-He Chen, Haolin Lu, Zhenzhen Wu, Hao Wang, Shanqing Zhang, Shilin Mei, Guankui Long, Qichun Zhang*, and Chang-Jiang Yao*

Experimental Section

Materials and Characterization

All starting chemicals and solvents were obtained from Energy Chemical or MREDA, and used without further purification. Proton magnetic resonances (^{1}H NMR) were conducted on Bruker Avance III 400MHz. Transform Infrared Spectroscopy (FT-IR) was recorded with Bruker 46 TENSOR Π. Thermal gravimetric analysis (TGA) was carried out with NETZSCH STA449F3 at a heating rate of 10 °C min^{-1} under nitrogen atmosphere. The microstructure and morphology were observed by high-resolution cold field-emission scanning electron microscopy (SEM, Regulus 8230) equipped with energy dispersive spectroscopy (EDS) for elemental analysis. Elemental analysis (EA) was conducted on a PerkinElmer 2400Series II CHNS/O elemental analyzer.

Synthesis of the PTO-2Br

PTO-2Br was synthesized according to literatures[1], and light-yellow powder was obtained with the yield of 87%. ^{1}H NMR (300 MHz, CDCl$_3$, δ): 8.60 (s, 4H, Ar H).

Synthesis of compound 1

To 20 mL ethylene glycol and 20 mL toluene were added PTO-2Br (844 mg, 2 mmol) and TsOH.H$_2$O (760 mg, 4 mmol). The mixture was heated at 140 °C for 36 h under argon protection. After the solution cooled down to room temperature, the product was purified by filtration and washing with water and EtOH to yield 937 mg of compound **1**, as a white powder in 80.5% yield. ^{1}H NMR (300 MHz, CDCl$_3$, δ): 7.89 (s, 4H), 4.21

(s, 8H), 3.67 (s, 8H).

Pyrene−4,5,9,10−tetraone (PTO), PTO-2Br and **1** were synthesized according to the reported methods.[2] As shown in Scheme. S1 and S2.
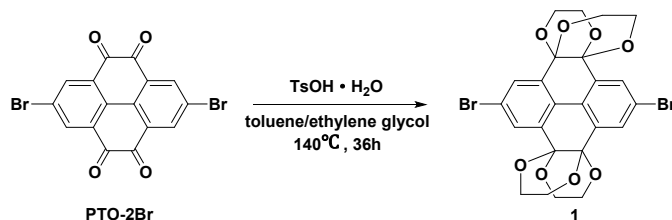
Scheme S1. Synthesize routes of compound **1**.
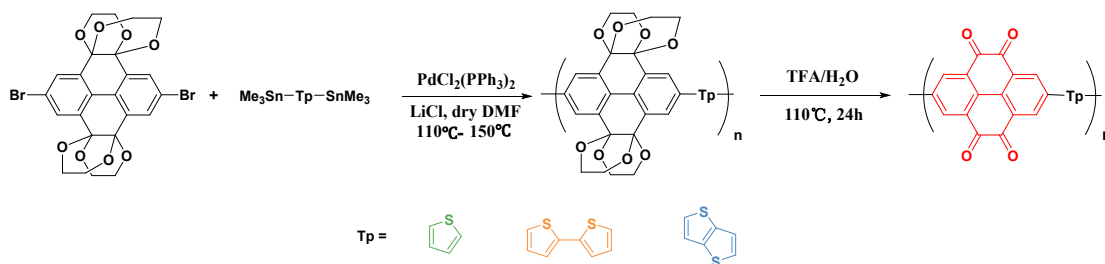
Scheme S2. The synthesis route of P(PTO-T1) P(PTO-T1) and P(PTO-T1) products.

Synthesis of P(PTO-TT)

To 10 mL of DMF were added compound **1** (119.2 mg, 0.2 mmol), 2,5-Bis(trimethylstannyl)thieno[3,2-b]thiophene (93.2 mg, 0.2 mmol), LiCl (84.8 mg, 2 mmol) and PdCl$_2$(PPh$_3$)$_2$ (11.2 mg, 0.016 mmol) in a 25 mL Schlenk tube. The mixture was heated at 110 °C for 12 h, 130 °C for 12 h and 150 °C for 72h under argon atmosphere. The system was then cooled to room temperature, and the precipitate was collected by filtration and washed successively with water and acetone to yield dark green powder. The obtained product was added into a mixture of TFA-H$_2$O (9:1, 10 ml) and refluxed in a sealed tube under argon protection for 24 hrs. The system was then cooled down to room temperature, after filtration, the filtrate washed with water and EtOH to yield black powder, where the soluble oligomer was removed by further

Soxhlet extraction with THF, DCM and acetone to yield 28.4 mg of **P(PTO-TT)**, as a black powder in yield of 35.5%. The element analysis of as-synthesized polymer: C 60.39%; H 2.19%; S 14.72%. Elemental Analysis: Calculated for $C_{113}H_{39}BrO_{20}S_{10}Sn$: C 60.71, H 1.76, S 14.34; found: C 60.39, H 2.19, S 14.72.

Synthesis of P(PTO-T2)

The compound **P(PTO-T2)** was synthesized using the same method as **P(PTO-TT)**. For this purpose, to 10 mL of DMF were added compound **1** (119.2 mg, 0.2 mmol), 5,5'-Bis(trimethylstannyl)-2,2'-bithiophene (94.8 mg, 0.2 mmol), LiCl (84.8 mg, 2 mmol) and $PdCl_2(PPh_3)_2$ (11.2 mg, 0.016 mmol) in a 25 mL Schlenk tube. By following the same preparation method as that of **P(PTO-TT)** and then the brown yellow powder was successfully obtained. After deprotecting with TFA-H_2O (9:1, 10 ml) for 24 hrs Soxhlet purification was performed with THF, DCM and acetone, then 57.3 mg of **P(PTO-T2)** was obtained, as a black powder in 67.2% yield. Elemental Analysis: Calculated for $C_{219}H_{81}BrO_{36}S_{18}Sn$: C 64.73, H 2.01, S 14.20; found: C 64.84, H 2.64, S 14.32.

Synthesis of P(PTO-T1)

The synthesis of **P(PTO-T1)** materials was the same as that of the **P(PTO-TT)**. For this purpose, to 10 mL of DMF were added compound **1** (119.2 mg, 0.2 mmol), 2,5-Bis(trimethylstannyl)thiophene (94.8 mg, 0.2 mmol), LiCl (84.8 mg, 2 mmol) and $PdCl_2(PPh_3)_2$ (11.2 mg, 0.016 mmol) in a 25 mL Schlenk tube. By following the same preparation method as that of P(PTO-TT) and then the dark yellow powder was successfully obtained. After deprotecting with TFA-H_2O (9:1, 10 ml) for 24 hrs, Soxhlet purification was performed with THF, DCM and acetone, then 58 mg of P(PTO-T1) was obtained, as a black powder in 84.2% yield. Elemental Analysis: Calculated for $C_{223}H_{75}BrO_{44}S_{11}Sn$: C 66.81, H 1.89, S 8.80; found: C 66.89, H 2.53, S 8.86.
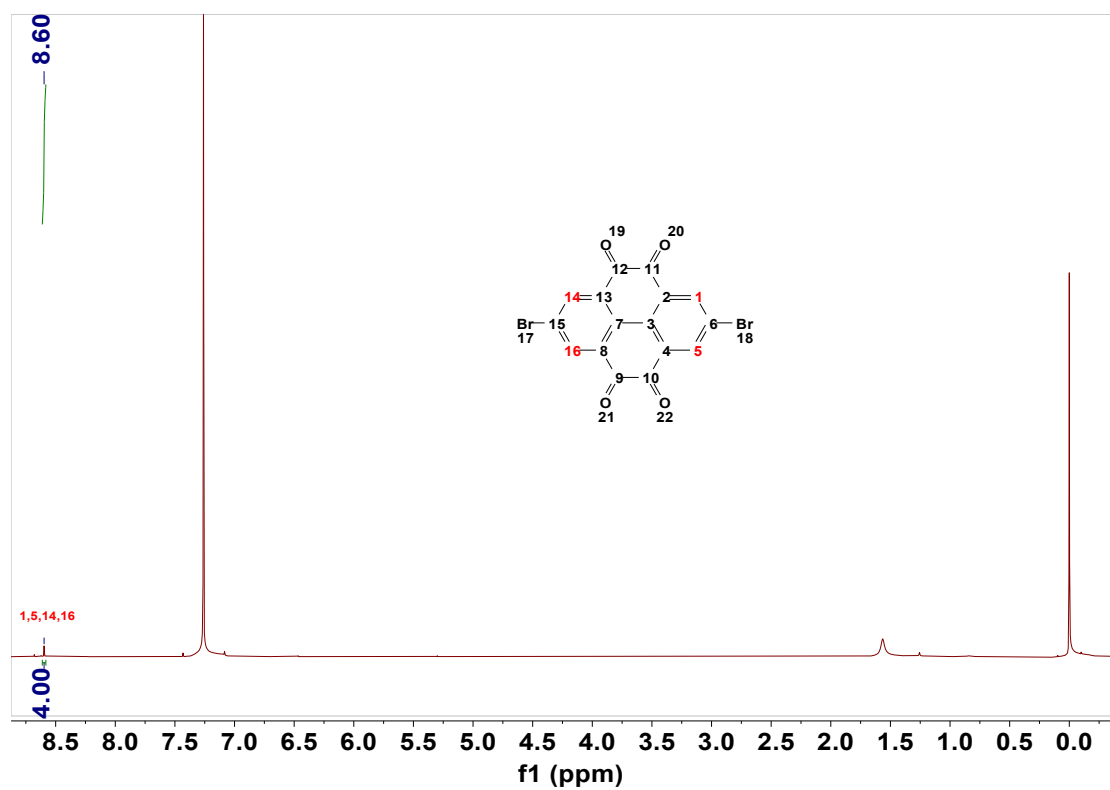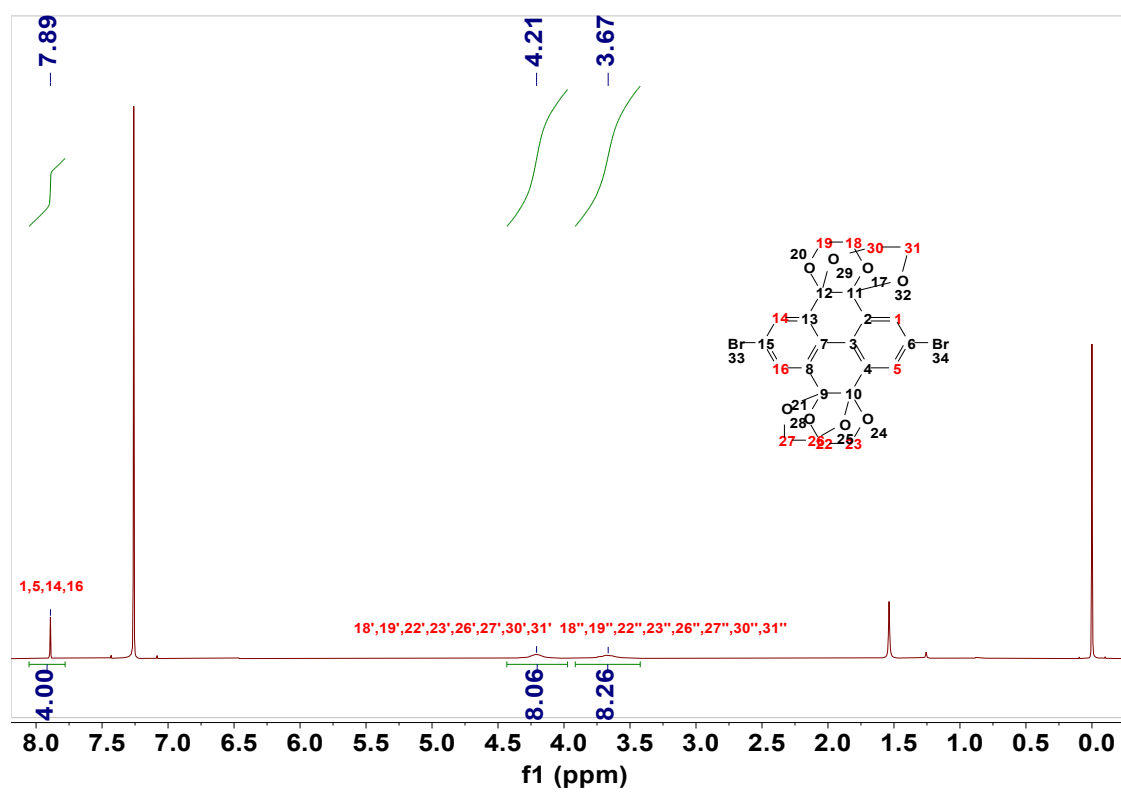
Figure S1. 1H NMR spectrum of PTO-2Br.

Figure S2. 1H NMR spectrum of compound **1**.

Electrode Preparation and Coin-Type Cell Fabrication

In order to investigate the electrochemical performance of P(PTO-T1), P(PTO-T2) and P(PTO-TT), the coin-type half-cells batteries with 1.0 M LiTFSI (DOL:DME=1:1) electrolyte were fabricated. The as-prepared P(PTO-T1), P(PTO-T2) and P(PTO-TT) polymers (each 15 mg) were mixed with carbon additives (Super P) (25 mg) and polymer binders (polyvinylidene fluoride) (10 mg) with a weight ratio of 3:5:2, using N-methyl-2-pyrrolidone (NMP) as solvent. After full grinding, homogeneous P(PTO-T1), P(PTO-T2) and P(PTO-TT) electrode slurries were separately obtained and uniformly coated on carbon-coating aluminum foils. The as-prepared electrode films were dried at 80 °C overnight in a vacuum atmosphere and then taken out. Finally, P(PTO-T1), P(PTO-T2) and P(PTO-TT) electrodes with diameters of 12 mm were separately punched and to be used. The mass loadings of active material are typically 1-1.6 mg per electrode. The lithium foils were used as the counter electrodes. Celgard 2325 membrane was applied as the separator and 1 mol/L (M) lithium bis(trifluoromethylsulphonyl)imide (LiTFSI) in 1,3-dioxolane/1,2-dimethoxyethane (DOL/DME) solvent (1/1, v/v) was used as the electrolyte. The cell was fabricated in a glove box filled with pure argon, in which the oxygen and water levels were both maintained below 1 ppm. Finally, the assembled cells were placed for an equilibration time of 12 h before separately test. Galvanostatic experiments were performed at different current densities at a potential range of 3.5 - 1.5 V (versus Li/Li$^+$) with a LANHE-CT2001A test system (Wuhan, China) at room temperature. CV were performed on the electrochemical workstation (CHI 660E) within a potential 1.5 - 3.5 V at the scan rates of 0.2 mV s^{-1}. EIS analysis was conducted by the same instrument between 100 kHz and 10mHz.

The electrodes for the ex-situ FT-IR test and SEM characterizations were prepared by grinding P(PTO-TT), carbon additives (Super P) and polymer binders (polyvinylidene fluoride) in a weight ratio of 7:2:1. Then, the slurry was uniformly coated on aluminum foils. After dried at 80 °C for 12 h under vacuum, the coin-type cell was assembled in

the Ar-filled glove box. The assembled cells for ex-situ FTIR measurements were cycled to a certain state of charge or discharge and disassembled in an Ar-filled glovebox. The electrodes were washed by DOL and dried in vacuum.
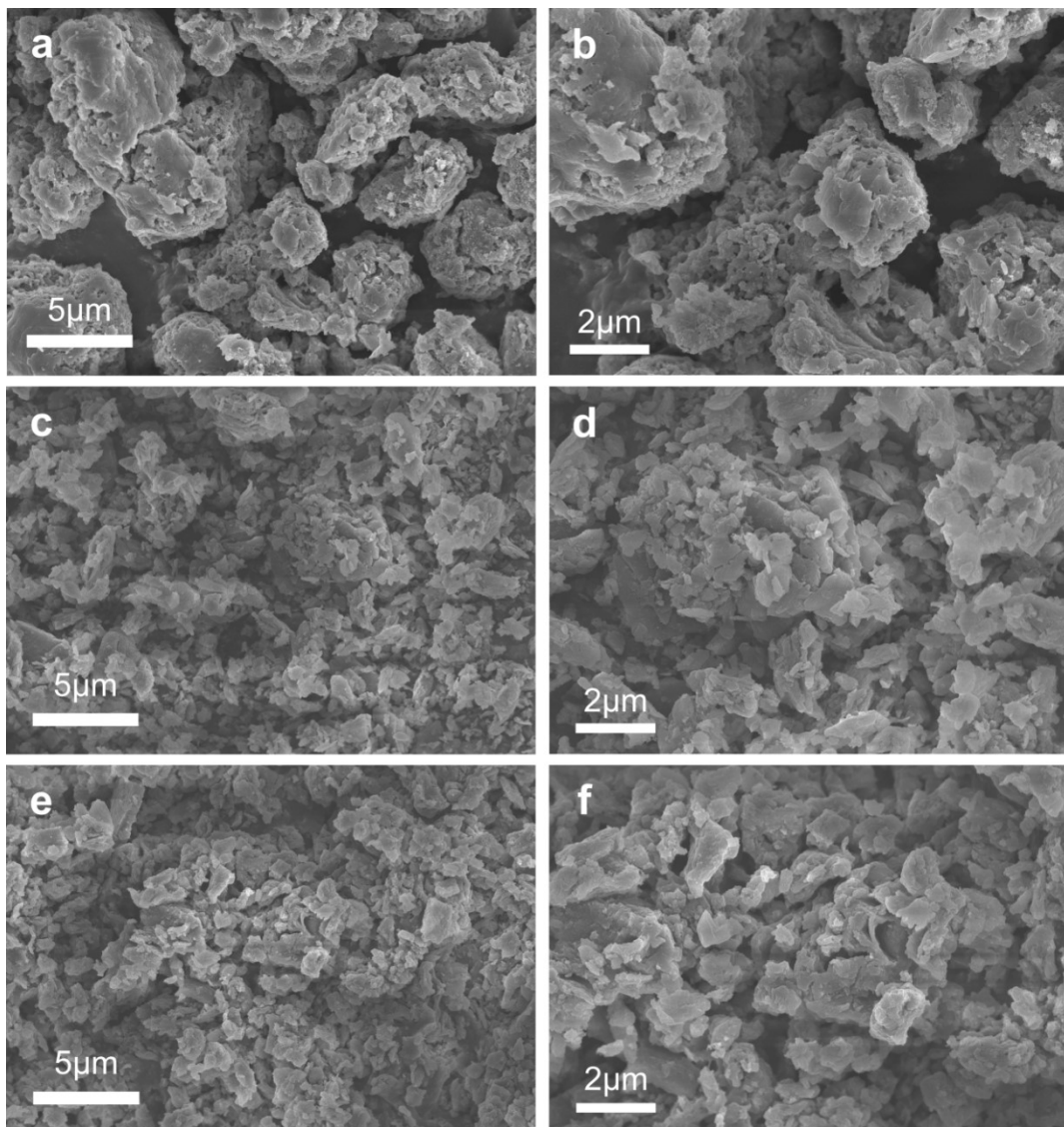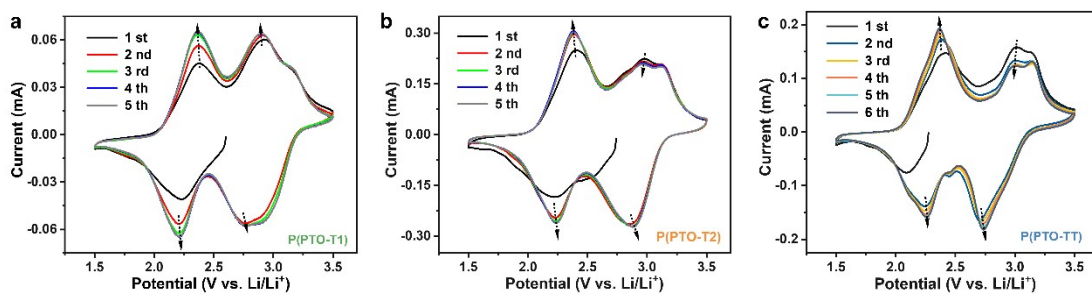

**Figure S3.** SEM images of as-prepared (a, b) P(PTO-T1), (c, d) P(PTO-T2) and (e,f) P(PTO-TT).
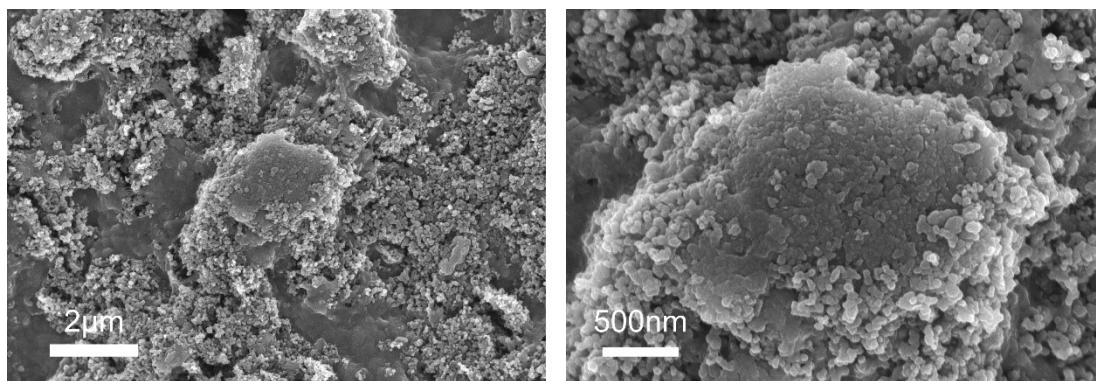
Figure S4. SEM images of pristine P(PTO-TT) cathode surface with different magnifications (after mixing with super P and PVDF).
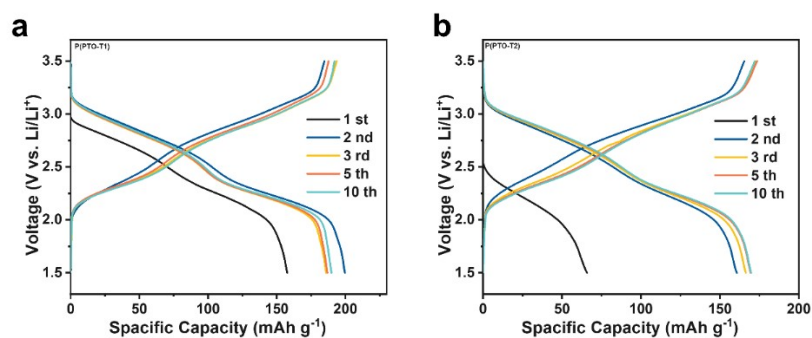
Figure S5. Galvanostatic charge–discharge profiles of (a) P(PTO-T1) and (b) P(PTO-T2) cathodes at 50 mA g^{-1}.

Figure S6. CV measurements of (a) P(PTO-T1), (b) P(PTO-T2) and (c) P(PTO-TT) cathodes at a scan rate of 0.2 mV s^{-1}.
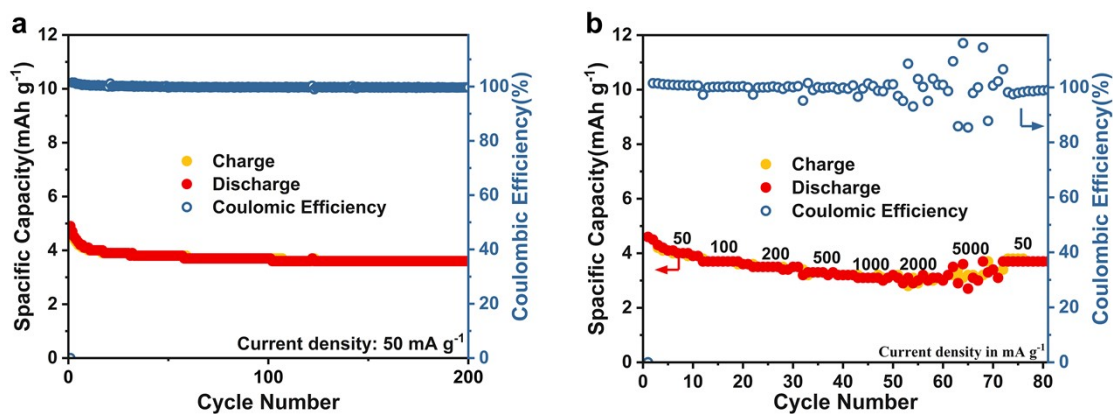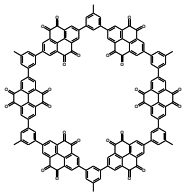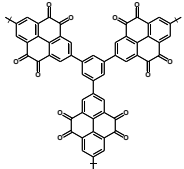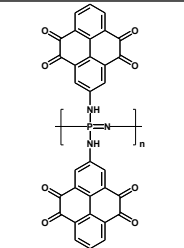
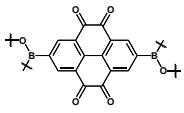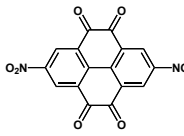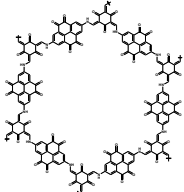**Figure S7.** (a) Cycling performance of super P electrodes (super P : PVDF = 8 : 2) at 50 mA g⁻¹ in 1.5–3.5 V. (b) Rate performance of super P electrodes at different current density.

Table S1. A comparison table includes several polymer electrodes for lithium-ion batteries.

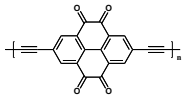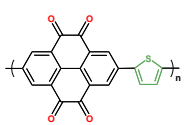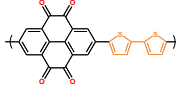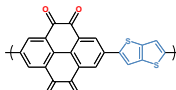| Molecular structure	Electrode composition	Electrolyte	Initial capacity (mA h g⁻¹) / current density or C rate / Cycle numbers / Capacity retention	Rate capacity (mA h g⁻¹)/current density [mA g⁻¹/C]	Ref.
	PPTO, CNT, PVDF (3:5:2)	1M LiTFSI in DOL/DME (1/1, v/v)	234 / 20 mA g⁻¹ / 100 cycles / 68.8%; 131 / 100 mA g⁻¹ / 953 cycles / 74.0%	131/0.1 A g⁻¹	2
	PEPTO, CNT, PVDF (3:5:2)	1 M LiTFSI in DOL/DME (1/1, v/v)	244 / 20 mA g⁻¹ / 100 cycles / 63.5%; 152 / 800 mA g⁻¹ / 953 cycles / 72.4%	152/0.8 A g⁻¹ 98/1.5 A g⁻¹	2
	PPYT, AB, PVDF (1.5:4:1)	LiNTf2/G4 at 45 °C	231 / 1C / 500 cycles / 83.5%	208/30 C	3

8

|					
	PT-BTA, AB, PVDF (30:60:10)	1 M LiTFSI in DOL/DME (1/1, v/v)	157 / 50 mA g^{-1} / 100 cycles / 95.5%; 128 / 200 mA g^{-1} / 500 cycles / 63.6%	93.1/1 A g^{-1}	4
	PPh-PTO, KB, PVDF (60:30:10)	1 M LiClO4/G4	224 / 100 mA g^{-1} / 1400 cycles / 98.2%	191/1 A g^{-1} 95/2 A g^{-1}	5
	PPAPT, KB 30:70	1 M LiPF$_6$ in EC/DMC (1:1, v/v)	156 / 20C (0.9 mA g^{-1}) / 500 cycles / 71.8%	192/1 C (45 mA g^{-1}) 156/20 C (0.9 A g^{-1})	6
	PPTODB, MWCNT (7:3)	LiPF$_6$ in EC/DMC (1:1, v/v)	198 / 20 mA g^{-1} / 150 cycles / 68.2%	133/1 A g^{-1} 98/1.5 A g^{-1}	7
	PT-2NO$_2$, AB, PVDF (4:5:1)	1 M LiTFSI in DOL/DME (1:1 v/v)	N/A / 50 mA g^{-1} / 120 cycles / N/A	104/1 A g^{-1}	8
	PT-COF50, Super C65, PVDF (70:20:10)	1 M LiTFSI in DOL/DME (1/1, v/v)	~232 / 2 A g^{-1} / 3000 cycles / 82%	229 / 5 A g^{-1}	9
	DE-PTO was dissolved in THF and dropped on a CNT paper	1 M LiPF6 in (EC/DMC, 1:1, v/v)	296 / 150 mA g^{-1} / 500 cycles / 177%; 248 / 300 mA g^{-1} / 1000 cycles / 165%	225/1.5 A g^{-1} 184/3 A g^{-1}	10
	P(PTO-T1), Super P, PVDF (30:50:20)	1 M LiTFSI in DOL/DME (1/1, v/v)	187 / 50 mA g^{-1} / 186 cycles / 92.5%; 63 / 2 A g^{-1} / 1200 cycles / 76.2%	96/1 A g^{-1} 72/2 A g^{-1}	This work

|	P(PTO-T2), Super P, PVDF (30:50:20)	1 M LiTFSI in DOL/DME (1/1, v/v)	172 / 50 mA g⁻¹ / 200 cycles / 83.7%; 92 / 2 A g⁻¹ / 1200 cycles / 81.5%	122 /1 A g⁻¹ 105/2 A g⁻¹	This work
	P(PTO-TT), Super P, PVDF (30:50:20)	1 M LiTFSI in DOL/DME (1/1, v/v)	182 / 50 mA g⁻¹ / 200 cycles / 85.2%; 117 / 2 A g⁻¹ / 1200 cycles / 94.8%	143/1 A g⁻¹ 129/2 A g⁻¹	This work
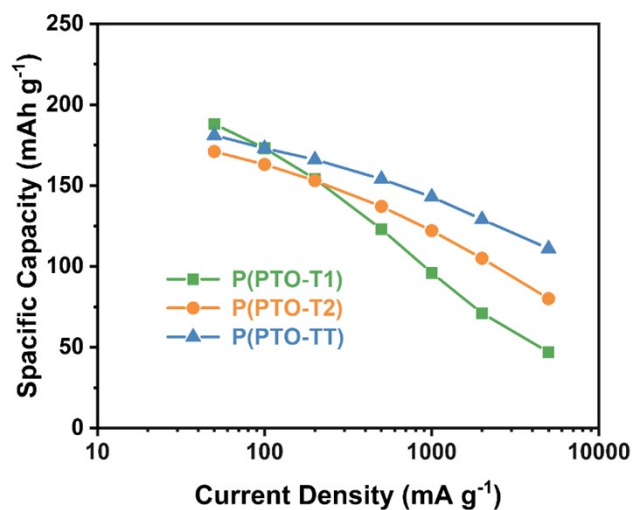
Figure S8. Specific capacity versus current density plots of the P(PTO-T1), P(PTO-T2) and P(PTO-TT) cathodes.
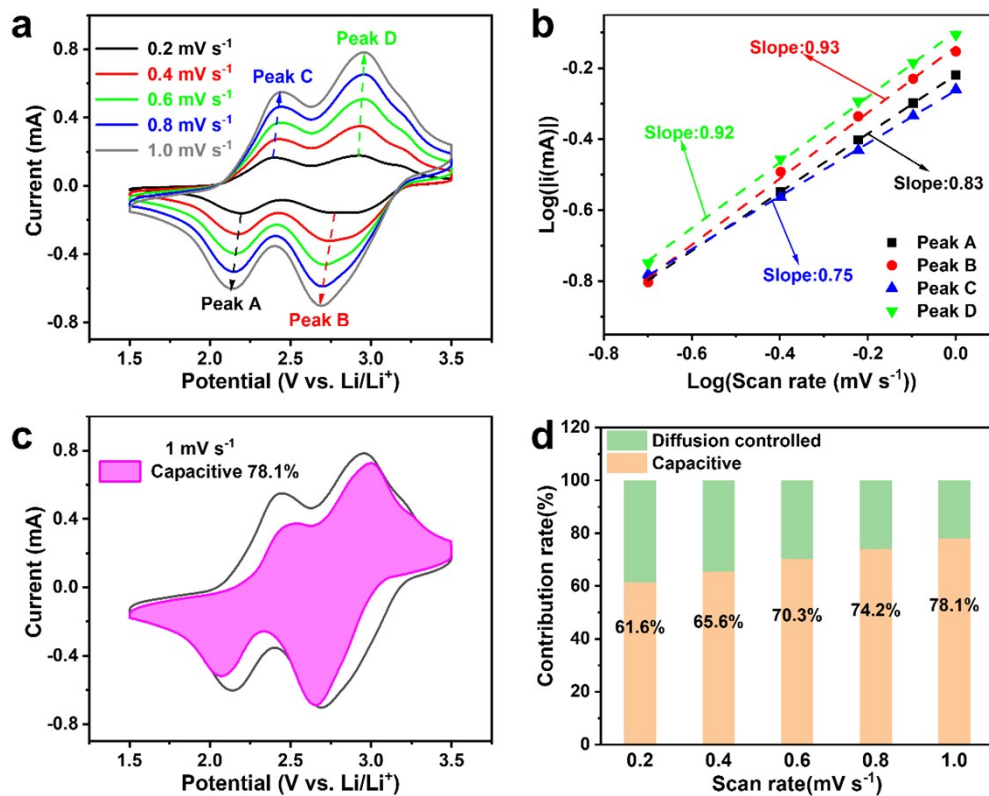
Figure S9. The reaction kinetics experiments of P(PTO-T1). (a) CV curves from a P(PTO-T1) electrode at different scan rates from 0.2–1.0 mV s^{-1}. (b) the relationship between log i and log v. (c) Capacitive and diffusion-controlled contributions at a scan rate of 1 mV s^{-1}. (d) The pseudocapacitive and diffusion-controlled charge storage contributions at different scan rates.
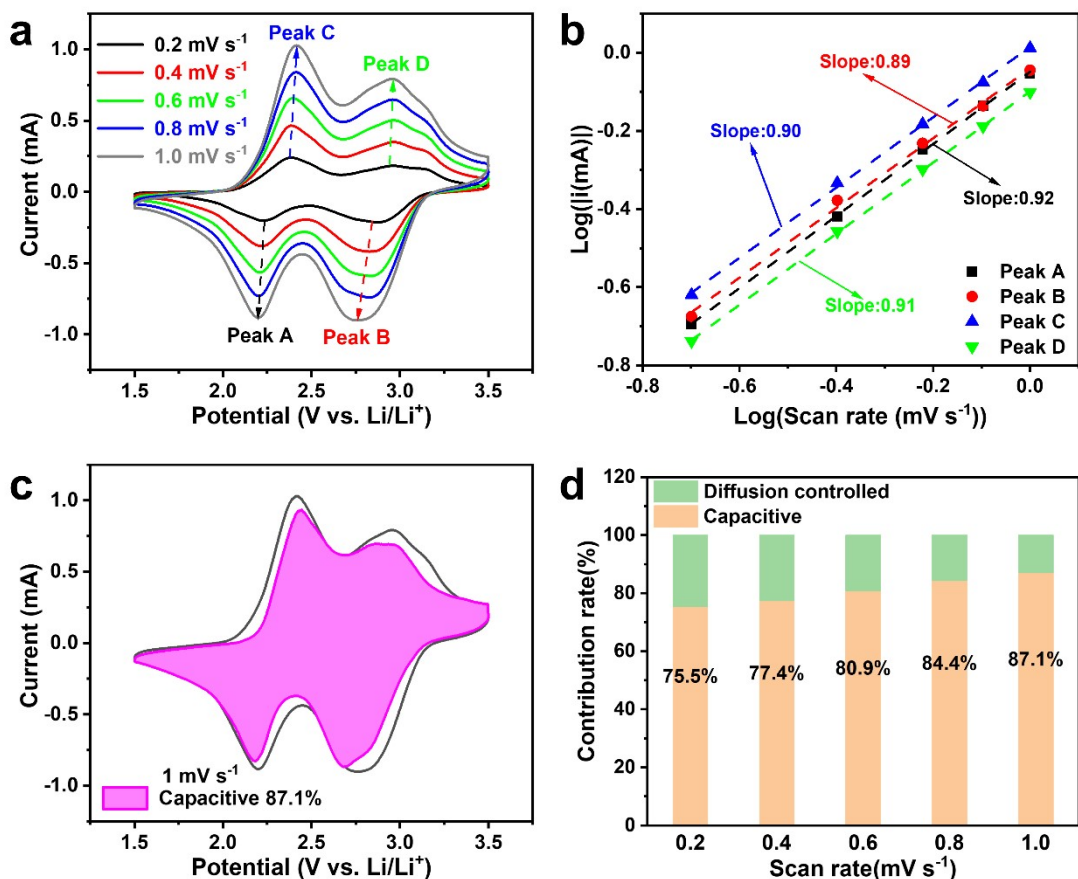
Figure S10. The reaction kinetics experiments of P(PTO-T2). (a) CV curves from a P(PTO-T2) electrode at different scan rates from 0.2–1.0 mV s^{-1}. (b) the relationship between log i and log v. (c) Capacitive and diffusion-controlled contributions at a scan rate of 1 mV s^{-1}. (d) The pseudocapacitive and diffusion-controlled charge storage contributions at different scan rates.

Table S2. The calculated Warburg impedance coefficient (σ_w) of P(PTO-T1), P(PTO-

T2) and P(PTO-TT) after 1 and 200 cycles.

	σ_w	
	1st cycle	200th cycle
P(PTO-T1)	23.7	140.3
P(PTO-T2)	38.0	156.4
P(PTO-TT)	26.9	67.1

Theoretical calculation

The Vienna Ab-initio Simulation Package (VASP) software[11,12] was used to accomplish the density functional theory (DFT) calculations. Geometric structures were relaxed until the total forces were smaller than 0.001 eV/Å. The projector augmented wave (PAW) method[13] with the Perdew-Burke-Ernzerhof (PBE) functional[14] was selected and the plane-wave cutoff energy was set to 530.0 eV. The polymers were arranged periodically in the form of one dimension with a vacuum of 20 Å. 1×1 Γ-centred Monkhorst-Pack mesh were used along the vacuum directions. For another direction, Γ-centered Monkhorst-Pack mesh k points with k-spacing of 0.02π Å^{-1} were employed for sampling the Brillouin zones for the static and density of states (DOS) calculations of three polymers. For the band structure calculation, 20 points were inserted between each pair of high symmetry k points. The VASPKIT[15] and AMSET[16] codes were used for post-processing analysis.

Table S3. The comparison of electronic conduction of polymers P(PTO-T1), P(PTO-T2) and P(PTO-TT)

	polymer	P(PTO-TT)	P(PTO-T2)	P(PTO-T1)
	Direction	X-Γ	Γ-X	Γ-X
m_e	CB	0.418	0.443	0.49
m_h	VB	-0.124	-0.137	-0.275

References

1 Q. Li, D. Li, H. Wang, H. Wang, Y. Li, Z. Si and Q. Duan, *ACS Appl. Mater. Inter.*, 2019, **11**, 28801–28808.

2 J. Xie, W. Chen, G. Long, W. Gao, Z. J. Xu, M. Liu and Q. Zhang, *J. Mater. Chem. A*, 2018, **6**, 12985-12991.

3 T. Nokami, T. Matsuo, Y. Inatomi, N. Hojo, T. Tsukagoshi, H. Yoshizawa, A. Shimizu, H. Kuramoto,

K. Komae, H. Tsuyama and J. Yoshida, *J. Am. Chem. Soc.*, 2012, **134**, 19694-19700.

4 K. Li, Q. Li, Y. Wang, H. Wang, Y. Li, Z. Si, *Materials Chemistry Frontiers*, 2020, **4**, 2697-2703.

5 S. Zheng, L. Miao, T. Sun, L. Li, T. Ma, J. Bao, Z. Tao and J. Chen, *J. Mater. Chem. A*, 2021, **9**, 2700-2705.

6 S. Yeşilot, N. Kılıç, S. Sariyer, S. Küçükköylü, A. Kılıç, R. Demir-Cakan, *ACS Applied Energy Materials*, 2021, **4**, 12487-12498.

7 C. Yao, Z. Wu, J. Xie, F. Yu, W. Guo, Z. J. Xu, D. Li, S. Zhang and Q. Zhang, *ChemSusChem*, 2020, **13**, 2457-2463.

8 Q. Li, H. Wang, H. Wang, Z. Si, C. Li and J. Bai, *ChemSusChem*, 2020, **13**, 2449-2456.

9 H. Gao, A. R. Neale, Q. Zhu, M. Bahri, X. Wang, H. Yang, Y. Xu, R. Clowes, N. D. Browning, M. A. Little, L. J. Hardwick and A. I. Cooper, *J. Am. Chem. Soc.*, 2022, **144**, 9434-9442.

10 H. Pan, Z. Zuo, F. He and Y. Li, *Energy Storage Mater.*, 2022, **52**, 465-472.

11 G. Kresse and J. Furthmülle, *Comp. Mater. Sci.*, 1996, **6**, 15-50.

12 Kresse and Furthmüller, *Physical review. B, Condensed Matter*, 1996, **54**, 11169.

13 P. E. Blöchl, *Physical Review B*, 1994, **50**, 17953.

14 P. P. John, R. Adrienn, I. C. Gabor, A. V. Oleg, E. S. Gustavo, A. C. Lucian, Z. Xiaolan and B. Kieron, *Phys. Rev. Lett.*, 2009, **102**, 039902.

15 V. Wang, N. Xu, J. C. Liu, G. Tang and W. T. Geng, *Comput. Phys. Commun.*, 2021, **267**, 108033.

16 A. M. Ganose, J. Park, A. Faghaninia, R. R. Woods, K. A. Persson and A. Jain, *Nat. Commun.*, 2021, **12**, 2222.